International Journal of Engineering

Efficient Removal of Copper Ion from Aqueous Solution using Crosslinked Chitosan Grafted with Polyaniline

H. Zare*[a], H. G. Taleghani[b], J. Khanjani[a]

[a] Department of Chemical, Materials and Polymer Engineering, Buein Zahra Technical University, Qazvin, Iran
[b] Faculty of Chemical Engineering, University of Mazandaran, Babolsar, Iran

PAPER INFO

A B S T R A C T

A high-performance adsorbent was produced by grafting polyaniline onto biopolymer chitosan. The morphological structure of cross-linked chitosan grafted with polyaniline was studied by scanning electron microscopy. Functional groups of the synthesized adsorbent were identified by Fourier-transform infrared. The performance of the prepared adsorbent was examined by batch adsorption experiments. The adsorption studies were performed with different operating parameters such as contact time, initial pH, adsorbent dosage and temperature. To evaluate adsorption isotherms, Freundlich, Langmuir and Dubinin-Radushkevich models were fitted to obtained data and the isotherm parameters were determined. Kinetics of the adsorption was studied by pseudo-first-order and pseudo-second-order models. It was observed that the obtained data were fitted more accurately with the pseudo-second-order model than the pseudo-first-order model. At optimum conditions, the maximum capacity and the removal efficiency of copper ions adsorption were obtained 131.58 mg/g and 92.5%, respectively. The regeneration efficiency and the removal efficiency of regenerated adsorbent were 97.7 and 90.4%, respectively. The results revealed the adsorbent has a great potential for adsorption of Cu (II) from aqueous solution.

doi: 10.5829/ije.2021.34.02b.01

1. INTRODUCTION

Heavy metals removal from wastewater is a global issue since they are the most dangerous environmental pollutants. Various industries, especially metal finishing, electroplating, plastics, battery, and etching are continuously releasing copper in their discharges [1-4]. Copper is an essential trace element but its concentration in air, water, and food should be below the tolerance limits; otherwise, it would be harmful to humans and animals. Intake of copper can lead to health complications such as causes irritation, mucosal, hepatic, lung cancer and capillary damage [3, 5, 6].

In recent years, various treatment procedures have been established for the removal of heavy metal ions. Currently, treatment processes include precipitation, oxidation-reduction, ion exchange, membrane filtration-osmosis, coagulation-flocculation, and adsorption. Each technique has its advantages and disadvantages, but the

adsorption method has been widely employed due to its simplicity of design and operation, low cost, high removal efficiency, and ease of adsorbent regeneration [7, 8].

Chitosan is a biopolymer with the linear structure of β-(1-4)-2amino-2-dexy-D-glucopyranose. Chitosan is generally produced by the deacetylation of chitin found in fungal cell walls and the exoskeleton of arthropods including insects, arachnids, and crustaceans (lobsters, crabs, and shrimps) [9-11]. Chitosan has potential to be employed in a diversity of fields, particularly in wastewater treatment. Chitosan is an appropriate adsorbent for the removal of heavy metals owing to the hydroxyl and amine functional groups [12, 13]. Chitosan has low mechanical strength and thermal stability and also it is soluble in acidic conditions [14, 15]. Several chemical and physical procedures have been applied to improve chitosan properties. Chemical modifications such as crosslinking and grafting improved porosity,

*Corresponding Author Institutional Email: hv.zare@bzte.ac.ir (H. Zare)

surface area, and mechanical properties of chitosan [16, 17].

In the current research, an appropriate adsorbent was made for removing Cu (II) from aqueous phase. In order to modify chitosan properties, chitosan was crosslinked by glutaraldehyde. Then crosslinked chitosan was grafted with polyaniline. The impact of initial pH, contact time, temperature, and adsorbent dosage were investigated. The resulted data were assessed by Freundlich and Langmuir isotherm models. Also, the adsorption kinetics were studied by pseudo-first-order (PFO) and pseudo-second-order (PSO) models.

2. MATERIALS AND METHODS

2. 1. Materials   Aniline, ammonium persulfate, acetic acid, citric acid, CuSO$_4$.5H$_2$O, and glutaraldehyde (50 wt% in H$_2$O) were purchased from Merck (Darmstadt, Germany). chitosan (85% deacetylated) were purchased from Sigma-Aldrich (St. Louis, Mo., USA). Stock solution of 1 g/l of Cu (II) was prepared using analytical grade CuSO$_4$.5H$_2$O and kept at ambient temperature. Desired concentrations of Cu ions were prepared by diluting the stock solution with double distilled water.

2. 2. Adsorbent Preparation   Chitosan was firstly dissolved in a solution of 2.5% acetic acid. Then 1.5% glutaraldehyde was poured into the chitosan solution and the obtained mixture stirred at 150 rpm for 5 h. Glutaraldehyde crosslinks chitosan chains by connecting amine groups. 2% aniline monomer in 50 ml of 1 M citric acid was added to the crosslinked chitosan solution. Then 5 ml of 10% ammonium persulfate was added to the solution drop by drop and stirred at 150 rpm for 10 h. In order to remove oligomers and impurities, cross-linked chitosan grafted with polyaniline (CCGP) was filtered and washed with acetone and double-distilled water. Finally, the resulted composite was completely dried in an oven at 60 °C for about 24 h.

2. 3. Batch Adsorption Experiments   To investigate the impact of operating conditions on Cu (II) adsorption, experiments were conducted in batch mode. Adsorption isotherm and kinetic evaluations were conducted for the adsorption process. Adsorption experiments were carried out with an initial concentration of 100 mg/l Cu (II) on a heater stirrer (IKA, Germany) at 300 rpm. Batch experiments for the elimination of Cu (II) from aqueous solution were conducted in a pH range of 2-6, adsorbent dosage of 1-5 g/l, and at various temperature in the range of 20 to 40 °C. The initial pH of the solution was set with addition of HCl solution for the required pH value. The initial pH of the solution was determined with a pH meter (AZ 86502,

Taiwan). Sampling was performed at specified time intervals, and Cu (II) concentration was determined by inductively coupled plasma optical emission spectrometry (ICP-OES, Varian 730-ES, USA). The Cu (II) removal efficiency, Re (%), was determined according to the following relation:

$$Re = \frac{C_i - C_t}{C_i} \times 100 \qquad (1)$$

where C_i is the initial Cu (II) concentration (mg/l), and C_t is the concentrations of Cu (II) at a given time (mg/l). q is the adsorption capacity, which is the Cu (II) amount adsorbed per unit mass of the adsorbent (mg/g). At a certain contact time of t, q_t (mg/g) was obtained by means of the equation below:

$$q_t = (C_i - C_t) \times \frac{V}{m} \qquad (2)$$

where V and m were the solution volume (1) and the adsorbent dosage (g), respectively.

2. 4. Characterization   Fourier-transform infrared (FTIR) spectra were acquired with a FTIR spectrometer (Bruker Tensor, Germany). The dried samples were milled into powder. One mg of each sample was blended with 100 mg of spectrophotometric grade KBr in an agate mortar and pressed into a tablet. FTIR spectra were recorded in the wavelength range of 400 to 4000 cm^{-1}. In order to study the surface morphology, the prepared CCGP was gold-coated with a sputtering coater (Emitech K575X, England), and the CCGP surface was observed by scanning electron microscope (SEM) (Phenom-ProX Sem, Netherlands).

3. RESULTS AND DISCUSSION

3. 1. FTIR Analysis   Functional groups of prepared CCGP were studied using FTIR (Figure 1). The IR spectra of CCGP showed an absorption band at 3439 cm^{-1} due overlapping the stretching vibration bands of both hydroxyl (–OH) and amine (–NH) groups [18]. The peaks at 2847 and 2923 cm^{-1} were attributed to the asymmetric and symmetric stretching vibrations of –CH$_2$ groups [19]. The peak at 1642 cm^{-1} corresponds to the stretching vibration of the C=O band of acetyl groups of chitosan remained in the adsorbent [3, 20]. The peak appearing at 1553 cm^{-1} associated with the nitrogen quinone, and the peak at 1456 cm^{-1} attributed to the benzene ring confirms the formation of polyaniline [21, 22]. The absorption band at 1310 cm^{-1} is due to the C–N stretching vibration of the benzenoid unit [23].

3. 2. SEM and EDAX Analysis   In order to investigate surface morphology of CCGP, scanning electron microscopy (SEM) image was taken at a magnification of 27500x (Figure 2). According to the

SEM image, CCGP contains particles smaller than 500 nm and has a high specific surface area. The large contact surface area between adsorbent and metal ions allows a large amount of adsorption relative to the weight of the adsorbent. EADX analysis of CCGP were performed before and after adsorption of copper ions (Figure 3). The presence of copper peak after adsorption indicates that copper ions were successfully adsorbed onto the CCGP.

3. 3. Effect of Contact Time   One of the effective parameters in the adsorption experiments is the contact time. Effect of contact time was studied with Cu (II) concentration of 100 mg/l, adsorbent dosage of 5 g/l, initial pH of 6 and at temperature of 20 °C for 180 min. Figure 4 presents the impact of time on the elimination of Cu (II) from the aqueous phase by the CCGP. The adsorption process reached to equilibrium after 100 min of contact time. At equilibrium time of 100 min, removal efficiency of 84.1% achieved and then remained almost constant.

3. 4. Effect of pH   The pH of the solution is recognized as the greatest significant parameter affecting
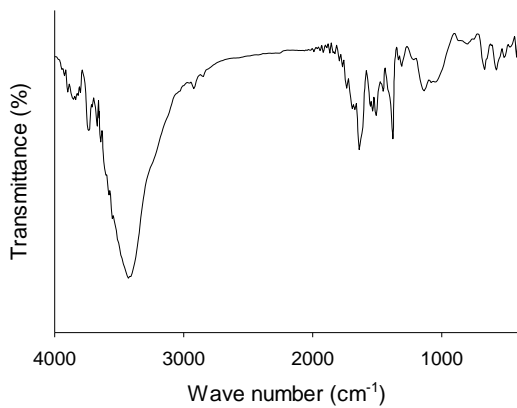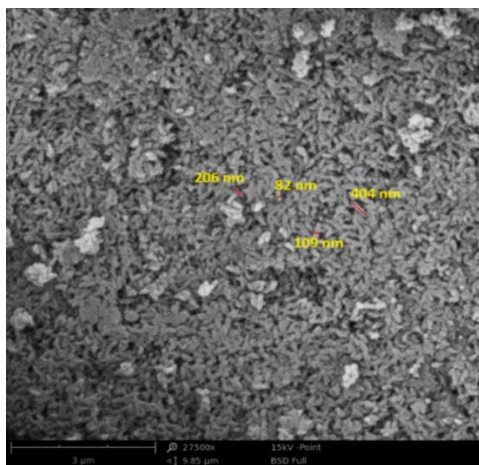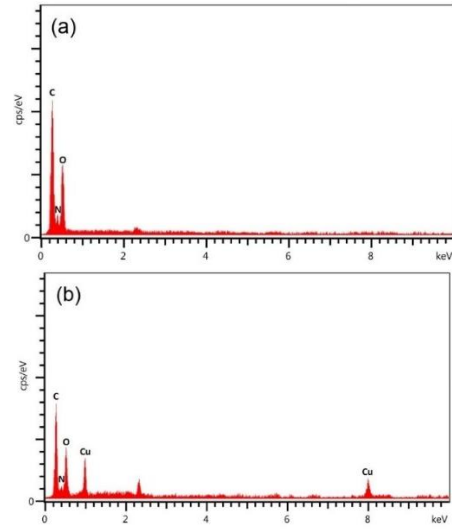

Figure 3. EADX analysis (a) before and (b) after adsorption of copper ions onto the CCGP

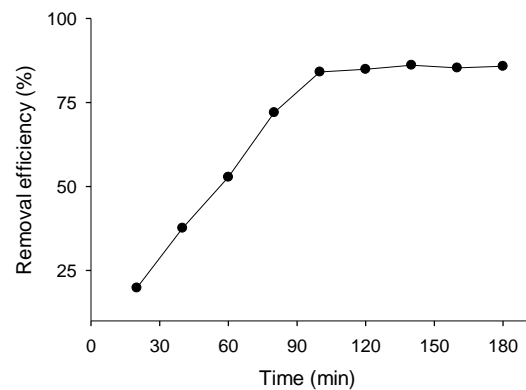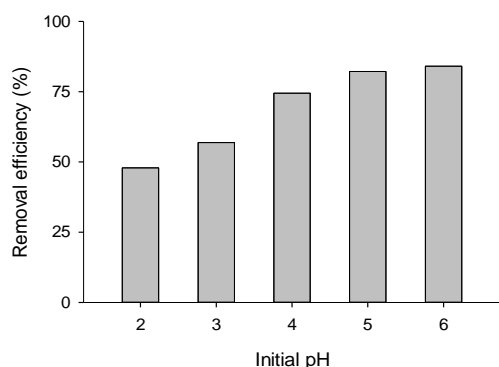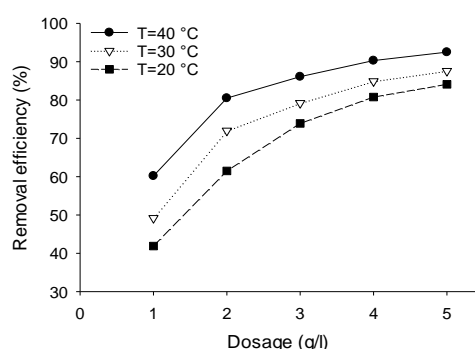**Figure 1.** FTIR spectra of the CCGP

Figure 4. The removal efficiency of Cu (II) ions by CCGP versus contact time, (Cu (II) concentration=100 mg/l, adsorbent dosage=5 g/l, initial pH=6, T=20 °C)

metal ions adsorption. To investigate the effect of pH on the adsorption process, the experiments were conducted at initial pH range of 2 to 6. At pH above 6, hydrate structures of copper are formed and the Cu (II) ions precipitate in the solution. Figure 5 presents the impact of pH on the removal of Cu (II) from solution by the CCGP. It can be perceived that the adsorbed amount of metal ions decreased with decreasing pH of solution. This is because at low pH values the amount of H^+ ions is high and therefore protons can contend with the copper cations for surface sites of the adsorbent. The removal efficiency was reached to maximum value at pH=6; therefore, further experiments were performed with an initial pH of 6.

3. 5. Effect of Temperature and Dosage of Adsorbent   The impact of adsorbent dose was investigated within the range of 1 to 5 g/l of the

Figure 2. SEM image of CCGP with magnification of 27500x

Figure 5. Impact of initial pH on the removal efficiency, (contact time=100 min, T=20 °C and adsorbent dosage=5 g/l)

Figure 6. Removal efficiency of Cu (II) at the adsorbent dosage of 1–5 g/L and temperature of 20–40 °C

adsorbent. The adsorption experiment was conducted at an optimum pH of 6 with the Cu (II) concentration of 100 mg/l. The experiments were carried out under isothermal conditions at various temperatures of 20, 30, and 40 °C. According to curves depicted in Figure 6, as the CCGP dosage increased, the Cu (II) adsorption onto the CCGP rapidly increased. When the adsorbent dose increases, the amount of available surface area increases, resulting in enhanced absorption of copper ions. Also, with increasing adsorbent dosage, the removal efficiency of Cu (II) increased. Maximum removal efficiency (92.5%) was obtained at an adsorbent dosage of 5 g/l and a temperature of 40°C.

3. 6. The Isotherm Models   Isotherms study the association between metal ions concentration in aqueous phase and the metal ions adsorbed onto the adsorbent at a constant temperature. The Langmuir model, a widely used isotherm, is suitable for investigating the adsorption of a monolayer on a surface containing a limited number of adsorption sites, which is given in the equation as follows [24]:

$$Re = \frac{q_{max}K_L C_e}{1+K_L C_e} \qquad (3)$$

The linear form of the Langmuir equation can be rearranged as shown below [25]:

$$\frac{C_e}{q_e} = \frac{1}{(K_L q_{max})} + \frac{C_e}{q_{max}} \qquad (4)$$

where C_e (mg/l) is the equilibrium concentration of Cu (II) in the aqueous phase, q_e (mg/g) is the Cu (II) amount adsorbed per unit mass of the adsorbent at equilibrium, q_{max} (mg/g) is the maximum capacity of adsorption at a given temperature, and K_L (L/mg) is the Langmuir constant. The plots of the adsorption isotherm fitted by the Langmuir equation are presented in Figure 7. The values of maximum capacity of the adsorption, q_{max}, and the Langmuir isotherm constants, K_L, were determined from the linear plots (Table 1).
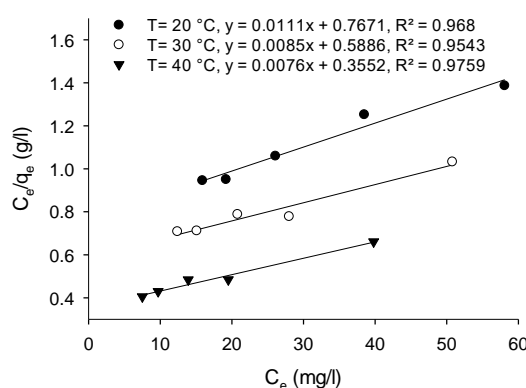
The empirical Freundlich isotherm model was extensively used to define the equilibrium adsorption data for a heterogeneous surface. The nonlinear form of the Freundlich model is expressed by the following equation [26]:

$$q_e = K_F(C_e)^{(1/n)} \qquad (5)$$

when the Freundlich equation is rearranged in logarithmic form, a linear equation of log (q_e) versus log (C_e) is obtained as follows [27]:

$$\log (q_e) = \log (K_F) + \left(\frac{1}{n}\right)\log (C_e \qquad (6)$$

where K_F is the Freundlich isotherm constant ((mg/g)/(mg/L)^n) which is associated to the adsorption capacity, and n is the adsorption intensity parameter. The plot of log (q_e) against log (C_e) is drawn according to the experimental adsorption data (Figure 8). Freundlich isotherm parameters were determined, which are summarized in Table 1. Depending on the results of adsorption isotherms, the maximum capacity of adsorption was obtained 131.58 mg/g at temperature of 40 °C. Also, the comparison of isotherm models showed that the experimental data were fitted better with Freundlich model than the Langmuir model.

Figure 7. The Cu (II) adsorption isotherm data fitted by Langmuir model at various temperatures of 20–40 °C, (Cu (II) concentration=100 mg/l, initial pH=6, contact time=100 min)

To investigate the mechanism of the adsorption of Cu (II) ions on the CCGP, Dubinin-Radushkevich (D-R) model was applied. The D-R model is given in linear form as follows [28]:
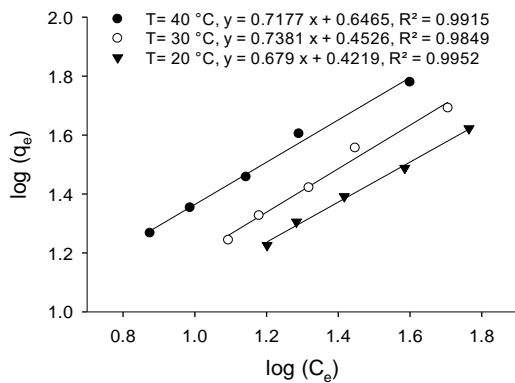
$$\ln(q_e) = \ln(q_s) - \beta\varepsilon^2 \tag{7}$$

In above equation, q_e is the mol of copper ions adsorbed per unit mass of the adsorbent at equilibrium (mol/g), q_s is the isotherm saturation capacity (mol/g), β is the D-R isotherm constant related to adsorption energy (mol^2/J^2), and ε is the Polanyi potential that can be calculated by the following equation:
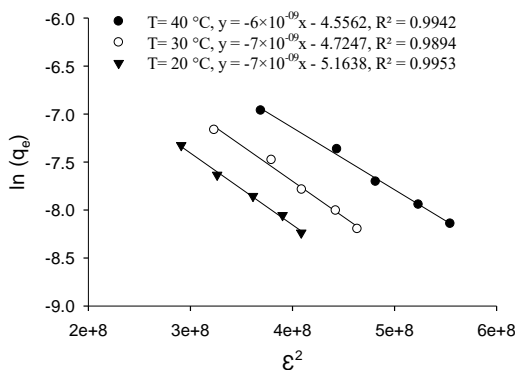
$$\varepsilon = RT \ln\left[1 + \frac{1}{C_e}\right] \tag{8}$$

The mean free energy E (J/mol) of the adsorption process depends on β, which is calculated by the following equation:

$$E = \frac{1}{\sqrt{2\beta}} \tag{9}$$

Figure 8. The Cu (II) adsorption isotherm data fitted by Freundlich model at various temperatures of 20–40 °C, (Cu (II) concentration=100 mg/l, initial pH=6, contact time=100 min)

Figure 9. The Cu (II) adsorption isotherm data fitted by D-R model at various temperatures of 20–40 °C, (Cu (II) concentration=100 mg/l, initial pH=6, contact time=100 min)

The amount of E value is useful to determine the mechanism of the adsorption process. The E values between 8 and 16 kJ/mol indicate that chemical interaction is the mechanism of the adsorption. If the value of E is less than 1, physical absorption is the dominant mechanism [29]. The plot of ln (q_e) versus ε^2 is depicted in Figure 9. The D-R isotherm parameters are listed in Table 1. The E values obtained from D-R isotherm model showed that chemical adsorption is the dominant mechanism of the copper ions adsorption onto the CCGP.

3. 7. Adsorption Kinetics   Adsorption kinetics was employed to investigate the diffusion of adsorbate into the adsorbent by measuring the adsorption uptake regarding the time at a constant concentration. In order to study the adsorption kinetics, the batch experiment was carried out at a pH of 6, a temperature of 40 °C and an adsorbent dosage of 5 g/l for 180 min (Figure 10a). PFO and PSO models were applied to study adsorption kinetics of Cu (II) by the adsorbent.

The PFO kinetic model for Cu (II) adsorption on the adsorbent was evaluated by incorporating the experimental adsorption data into the following equation [30]:

$$\log(q_e - q_t) = \log q_e - \frac{k.t}{2.303} \tag{10}$$

where q_e (mg/g) is the equilibrium amount Cu (II) adsorbed per unit mass of the adsorbent, and k (min^{-1}) is the PFO rate constant. The rate constant value, k, is determined from the linear plot (Figure 10b). The values of the PFO rate constant and the correlation coefficient were k = 0.042 min^{-1} and 0.882, respectively.

The differential equation of PSO kinetic model is represented as follows [31]:

$$\frac{dq_t}{dt} = K(q_e - q_t)^2 \tag{11}$$

TABLE 1. Isotherm specifications of the Freundlich and Langmuir models for the adsorption of Cu (II) ions on the CCGP

Isotherm models	Parameters	Temperature (°C)		
		20	**30**	**40**
Langmuir	K_L (L/mg)	0.0145	0.0161	0.0214
	q_m (mg/g)	90.09	108.70	131.58
	R^2	0.968	0.954	0.976
Freundlich	K_F ((mg/g)/(mg/L)^n)	2.64	2.84	4.43
	n	1.47	1.35	1.39
	R^2	0.995	0.985	0.992
D-R	E (kJ/mol)	8.452	8.452	9.129
	R^2	0.995	0.989	0.994

PSO model can be written to linear form for the convenience of plotting and determining rate constant as following equation [32]:

$$\frac{t}{q_t} = \frac{1}{Kq_e^2} + \frac{t}{q_e} \qquad (12)$$

where q_t (mg/g) is the Cu (II) amount adsorbed per the mass of the adsorbent at a contact time of t (min). K (g mg^{-1} min^{-1}) represents the kinetic rate constant that depends on the conditions of the copper adsorption process on the adsorbent. The adsorption kinetics plot fitted by PSO is shown in Figure 10c. The PSO rate constant, k = 6.06×10^{-5} g mg^{-1} min^{-1} was determined from the linear plot with the correlation coefficient of 0.983. Based on the results, for the absorption of copper ions onto CCGP, PSO kinetic model was more suitable than PFO model.

Figure 10. (a) Removal efficiency of Cu (II) (initial concentration = 100 mg/l, pH = 6, adsorbent dosage = 5 g/L, T = 40 °C, t = 180 min), (b) PFO kinetic model, and (c) PSO kinetic model for Cu (II) adsorption onto CCGP

3. 8. Regeneration and Reusability of the Adsorbent   Regeneration and reusability of the CCGP saturated with copper ions was studied after five consecutive adsorption-desorption cycles. For each adsorption-desorption cycle, CCGP was soaked three times in succession in 0.5 ml HCl solution for 2 hours at 300 rpm. The CCGP was filtered and washed with double-distilled water after each soak. The adsorption experiments were done again using the regenerated CCGP at optimum conditions. After one cycle of adsorption-desorption, the efficiency of CCGP regeneration and the removal efficiency of Cu (II) ions were 97.7 and 90.4%, respectively. After five adsorption-desorption cycles, the regeneration efficiency and the removal efficiency were 81.7 and 75.6%, respectively. Results showed that CCGP has good performance for regeneration and reusability.

Adsorption of Cu (II) ions from aqueous solution using CCGP was investigated. Maximum adsorption capacity (mg of metal ion adsorbed per gram of adsorbent) of CCGP for Cu (II) ions was 131.58 mg g^{-1}. The results were compared with other adsorbents reported in literature (see Table 2). It can be seen that the synthesized CCGP had the highest potential to remove heavy metals from aqueous solutions.

TABLE 2. Comparison of the maximum adsorption capacities of CCGP with other adsorbents

Adsorbent	Maximum adsorption capacity, mg/g	Reference
Chlamydomonas microsphaera collected by polyaluminium chloride flocculation	79.4	[33]
Magnetic chitosan	104	[34]
Carboxylated cellulose cryogel beads crosslinked by maleic anhydride	84.12	[35]
Functionalized graphene nanosheets	103.22	[36]
Chitosan-modified magnetic Mn ferrite nanoparticles	65.1	[37]
Calcium alginate with encapsulated graphene oxide	60.2	[38]
Epichlorohydrin cross-linked xanthate chitosan	43.47	[39]
Powdered activated carbon-magnetite nanoparticles	23.61	[40]
Spherical polystyrene-supported chitosan	99.8	[41]
CCGP	131.58	This study

4. CONCLUSION

Preparation of an efficient adsorbent by grafting polyaniline onto cross-linked chitosan was reported in this paper. The synthesized composite material CCGP has a high specific surface area with different functional groups, such as amine and hydroxyl, which can enhance the adsorption capacity for heavy metals. The removal efficiency of Cu (II) was dependent on the contact time, initial pH, temperature, and adsorbent dosage. The experimental data were appropriately fitted to Freundlich isotherm model and PSO model with good correlation coefficients. It was concluded that the synthesized adsorbent can effectively remove the copper ions from aqueous solutions.

5. ACKNOWLEDGMENT

6. REFERENCES

1. Al-Saydeh, S.A., El-Naas, M.H. and Zaidi, S.J., "Copper removal from industrial wastewater: a comprehensive review", *Journal of Industrial and Engineering Chemistry*, Vol. 56, (2017), 35-44. doi: 10.1016/j.jiec.2017.07.026

2. Karim, N., "Copper and human health-a review", *Journal of Bahria University Medical & Dental College*, Vol. 8, No. 2, (2018), 117-122.

3. Krstić, V., Urošević, T. and Pešovski, B., "A review on adsorbents for treatment of water and wastewaters containing copper ions", *Chemical Engineering Science*, Vol. 192, (2018), 273-287. doi: 10.1016/j.ces.2018.07.022

4. Mohamadi, S., Saeedi, M. and Mollahosseini, A., "Desorption kinetics of heavy metals (lead, zinc, and nickel) coexisted with phenanthrene from a natural high buffering soil", *International Journal of Engineering*, Vol. 32, No. 12, (2019), 1716-1725. doi: 10.5829/IJE.2019.32.12C.04

5. Shahrin, S., Lau, W.J., Goh, P.S., Jaafar, J. and Ismail, A.F., "Adsorptive removal of Cr(VI) and Cu(II) ions from water solution using graphene oxide-manganese ferrite (Gmf) nanomaterials", *International Journal of Engineering*, Vol. 31, No. 8, (2018), 1341-1346. doi: 10.5829/ije.2018.31.08b.24

6. Yao, Z.Y., Qi, J.H. and Wang, L.H., "Equilibrium, kinetic and thermodynamic studies on the biosorption of Cu (II) onto chestnut shell", *Journal of Hazardous Materials*, Vol. 174, No. 1-3, (2010), 137-143. doi: 10.1016/j.jhazmat.2009.09.027

7. Peng, W., Li, H., Liu, Y. and Song, S., "A review on heavy metal ions adsorption from water by graphene oxide and its composites", *Journal of Molecular Liquids*, Vol. 230, (2017), 496-504. doi: 10.1016/j.molliq.2017.01.064

8. Zhang, L., Zeng, Y. and Cheng, Z., "Removal of heavy metal ions using chitosan and modified chitosan: a review", *Journal of Molecular Liquids*, Vol. 214, (2016), 175-191. doi: 10.1016/j.molliq.2015.12.013

9. Rolandi, M. and Rolandi, R., "Self-assembled chitin nanofibers and applications", *Advances in Colloid and Interface Science*, Vol. 207, (2014), 216-222. doi: 10.1016/j.cis.2014.01.019

10. Roseman, S., Li, X. and Comb, D., "Conversion of chitin into N-acetylglucosamine, glucosamine and bioethanol", (2016), Google Patents.

11. Varalakshmi, V. and Mala, R., "Effect of herbal extract on antimicrobial susceptibility profile of drug resistant burn wound isolates", *International Journal of Agriculture, Environment and Biotechnology*, Vol. 6, No. 4S, (2013), 815.

12. Fan, C., Li, K., He, Y., Wang, Y., Qian, X. and Jia, J., "Evaluation of magnetic chitosan beads for adsorption of heavy metal ions", *Science of the Total Environment*, Vol. 627, (2018), 1396-1403. doi: 10.1016/j.scitotenv.2018.02.033

13. Gokila, S., Gomathi, T., Sudha, P. and Anil, S., "Removal of the heavy metal ion chromiuim (VI) using chitosan and alginate nanocomposites", *International Journal of Biological Macromolecules*, Vol. 104, (2017), 1459-1468. doi: 10.1016/j.ijbiomac.2017.05.117

14. Abraham, A., Soloman, P. and Rejini, V., "Preparation of chitosan-polyvinyl alcohol blends and studies on thermal and mechanical properties", *Procedia Technology*, Vol. 24, (2016), 741-748. doi: 10.1016/j.protcy.2016.05.206

15. Silina, N., Morozov, A., Gornostaeva, E., Smirnova, L. and Zaytsev, S., "Ultrasound-assisted synthesis of block copolymers of chitosan and D, L-lactide: structure and properties", *Polymer Science, Series B*, Vol. 59, No. 5, (2017), 551-559. doi: 10.1134/S1560090417050116

16. Acharyulu, S.R., Gomathi, T. and Sudha, P., "Physico-chemical characterization of cross linked chitosan-polyacrylonitrile polymer blends", *Der Pharmacia Lettre*, Vol. 5, No. 2, (2013), 354-363.

17. Mochalova, A. and Smirnova, L., "State of the art in the targeted modification of chitosan", *Polymer Science, Series B*, Vol. 60, No. 2, (2018), 131-161. doi: 10.1134/S1560090418020045

18. Moussout, H., Ahlafi, H., Aazza, M. and Bourakhouadar, M., "Kinetics and mechanism of the thermal degradation of biopolymers chitin and chitosan using thermogravimetric analysis", *Polymer Degradation and Stability*, Vol. 130, (2016), 1-9. doi: 10.1016/j.polymdegradstab.2016.05.016

19. Arumugam, T., Krishnamoorthy, P., Rajagopalan, N., Nanthini, S. and Vasudevan, D., "Removal of malachite green from aqueous solutions using a modified chitosan composite", *International Journal of Biological Macromolecules*, Vol. 128, (2019), 655-664. doi: 10.1016/j.ijbiomac.2019.01.185

20. Pires, C.T., Vilela, J.A. and Airoldi, C., "The effect of chitin alkaline deacetylation at different condition on particle properties", *Procedia Chem*, Vol. 9, (2014), 220-225. doi: 10.1016/j.proche.2014.05.026

21. Deng, J., Ding, X., Zhang, W., Peng, Y., Wang, J., Long, X., Li, P. and Chan, A.S., "Carbon nanotube–polyaniline hybrid materials", *European Polymer Journal*, Vol. 38, No. 12, (2002), 2497-2501. doi: 10.1016/S0014-3057(02)00165-9

22. Zhang, H., Zhao, Q., Zhou, S., Liu, N., Wang, X., Li, J. and Wang, F., "Aqueous dispersed conducting polyaniline nanofibers: promising high specific capacity electrode materials for supercapacitor", *Journal of Power Sources*, Vol. 196, No. 23, (2011), 10484-10489. doi: 10.1016/j.jpowsour.2011.08.066

23. Liu, W., Kumar, J., Tripathy, S., Senecal, K.J. and Samuelson, L., "Enzymatically synthesized conducting polyaniline", *Journal of the American Chemical Society*, Vol. 121, No. 1, (1999), 71-78. doi: 10.1021/ja982270b

24. Langmuir, I., "The adsorption of gases on plane surfaces of glass, mica and platinum", *Journal of the American Chemical society*, Vol. 40, No. 9, (1918), 1361-1403. doi: 10.1021/ja02242a004

25. Sasikala, S. and Muthuraman, G., "Removal of heavy metals from wastewater using tribulus terrestris herbal plants powder", *Iranica Journal of Energy and Environment*, Vol. 7, No. 1, (2016), 39-47. doi: 10.5829/idosi.ijee.2016.07.01.06

26 Freundlich, H., "Over the adsorption in solution", *The Journal of Physical Chemistry*, Vol. 57, (1906), 1100-1107.

27. Yavuz, A.G., Dincturk-Atalay, E., Uygun, A., Gode, F. and Aslan, E., "A comparison study of adsorption of Cr (VI) from aqueous solutions onto alkyl-substituted polyaniline/chitosan composites", *Desalination*, Vol. 279, No. 1-3, (2011), 325-331. doi: 10.1016/j.desal.2011.06.034

28. Dubinin, M.M., Zaverina, E. and Radushkevich, L., "Sorption and structure of active carbons. I. adsorption of organic vapors", *Zhurnal Fizicheskoi Khimii*, Vol. 21, No. 3, (1947), 151-162.

29. Sarı, A. and Tuzen, M., "Biosorption of cadmium (II) from aqueous solution by red algae (*Ceramium virgatum*): equilibrium, kinetic and thermodynamic studies", *Journal of Hazardous Materials*, Vol. 157, No. 2-3, (2008), 448-454. doi: 10.1016/j.jhazmat.2008.01.008

30. Rodrigues, L.A., Maschio, L.J., da Silva, R.E. and da Silva, M.L.C.P., "Adsorption of Cr (VI) from aqueous solution by hydrous zirconium oxide", *Journal of Hazardous Materials*, Vol. 173, No. 1-3, (2010), 630-636. doi: 10.1016/j.jhazmat.2009.08.131

31. Satapathy, M. and Das, P., "Assessment on the modelling of the kinetic parameter for the removal of crystal violet dye using Ag-soil nanocomposite: linear and non-linear analysis", *Desalination and Water Treatment*, Vol. 57, No. 9, (2016), 4073-4080. doi: 10.1080/19443994.2014.987179

32. Gao, A., Xie, K., Song, X., Zhang, K. and Hou, A., "Removal of the heavy metal ions from aqueous solution using modified natural biomaterial membrane based on silk fibroin", *Ecological Engineering*, Vol. 99, (2017), 343-348. doi: 10.1016/j.ecoleng.2016.11.008

33. Jiang, X., Zhou, X., Li, C., Wan, Z., Yao, L. and Gao, P., "Adsorption of copper by flocculated *Chlamydomonas microsphaera* microalgae and polyaluminium chloride in heavy metal-contaminated water", *Journal of Applied Phycology*, Vol. 31, No. 2, (2019), 1143-1151. doi: 10.1007/s10811-018-1636-6

34. Zhang, S., Zhou, Y., Nie, W., Song, L. and Zhang, T., "Preparation of uniform magnetic chitosan microcapsules and their application in adsorbing copper ion (II) and chromium ion (III)", *Industrial & Engineering Chemistry Research*, Vol. 51, No. 43, (2012), 14099-14106. doi: 10.1021/ie301942j

35. Tang, C., Brodie, P., Brunsting, M. and Tam, K.C., "Carboxylated cellulose cryogel beads via a one-step ester crosslinking of maleic anhydride for copper ions removal", *Carbohydrate Polymers*, Vol. No. (2020), 116397. doi: 10.1016/j.carbpol.2020.116397

36. Cao, M.-l., Li, Y., Yin, H. and Shen, S., "Functionalized graphene nanosheets as absorbent for copper (II) removal from water", *Ecotoxicology and Environmental Safety*, Vol. 173, No. (2019), 28-36. doi: 10.1016/j.ecoenv.2019.02.011

37. Meng, Y., Chen, D., Sun, Y., Jiao, D., Zeng, D. and Liu, Z., "Adsorption of Cu^{2+} ions using chitosan-modified magnetic Mn ferrite nanoparticles synthesized by microwave-assisted hydrothermal method", *Applied Surface Science*, Vol. 324, No. (2015), 745-750. doi: 10.1016/j.apsusc.2014.11.028

38. Algothmi, W.M., Bandaru, N.M., Yu, Y., Shapter, J.G. and Ellis, A.V., "Alginate–graphene oxide hybrid gel beads: An efficient copper adsorbent material", *Journal of Colloid and Interface Science*, Vol. 397, No. (2013), 32-38. doi: 10.1016/j.jcis.2013.01.051

39. Kannamba, B., Reddy, K.L. and AppaRao, B., "Removal of Cu (II) from aqueous solutions using chemically modified chitosan", *Journal of Hazardous Materials*, Vol. 175, No. 1-3, (2010), 939-948. doi: 10.1016/j.jhazmat.2009.10.098

40. Shahrashoub, M. and Bakhtiari, S., "The efficiency of activated carbon/iron oxide nanoparticles composites in copper removal: Industrial waste recovery, green synthesis, characterization, and adsorption-desorption studies", *Microporous and Mesoporous Materials*, Vol. No. (2020), 110692. doi: 10.1016/j.micromeso.2020.110692

41. Jiang, W., Chen, X., Pan, B., Zhang, Q., Teng, L., Chen, Y. and Liu, L., "Spherical polystyrene-supported chitosan thin film of fast kinetics and high capacity for copper removal", *Journal of Hazardous Materials*, Vol. 276, No. (2014), 295-301. doi: 10.1016/j.jhazmat.2014.05.032

Persian Abstract

چکیده

جاذبی با کارایی بالا با استفاده از پیوند دادن پلی آنیلین به بیوپلیمر کیتوسان تولید شد. ساختار مورفولوژی کیتوسان متصل شده عرضی و پیوند زده شده با پلی آنیلین توسط میکروسکوپ الکترونی روبشی بررسی شد. گروه‌های عاملی جاذب سنتز شده با استفاده از طیف سنجی مادون قرمز تبدیل فوریه شناسایی شد. عملکرد جاذب تهیه شده برای حذف یون‌های مس از محلول آبی با استفاده از روش ناپیوسته مورد تحقیق قرار گرفت. مطالعات جذب به عنوان تابعی از زمان تماس، pH اولیه، دما و میزان جاذب انجام شد. جهت ارزیابی ایزوترم جذب، مدل‌های لانگمویر، فروندلیچ و دوبینین رادوشکویچ برای داده‌های آزمایشگاهی برازش شد و پارامترهای ایزوترم تعیین گردید. سینتیک جذب توسط مدل‌های شبه درجه اول و شبه درجه دوم مورد مطالعه قرار گرفت. مشاهده شد که داده‌های آزمایشگاهی با مدل شبه درجه دوم بهتر از مدل شبه درجه اول برازش می‌شود. در شرایط بهینه حداکثر ظرفیت جذب و حداکثر راندمان حذف جاذب برای جذب Cu (II) به ترتیب ۱۳۱/۵۸ میلی گرم بر گرم و ۹۲/۵ درصد به دست آمد. راندمان احیای جاذب و راندمان حذف برای جاذب احیا شده به ترتیب ۹۷/۷ و ۹۰/۴ درصد شد. نتایج نشان داد جاذب سنتز شده پتانسیل بالایی برای حذف یون‌های مس از محلول آبی دارد.